View metadata, citation and similar papers at core.ac.uk

brought to you by CORE

東北大学機関リポジトリ TOUR Tohoku University Repository

A compact interferometer using moire effect for the phase compensation

著者	羽根 一博
journal or publication title	Review of scientific instruments
volume	63
number	8
page range	3856-3861
year	1992
URL	http://hdl.handle.net/10097/35574

doi: 10.1063/1.1143283

A compact interferometer using moire effect for the phase compensation

S. Watanabe and K. Hane
Department of Electronic-Mechanical Engineering, Nagoya University, Nagoya 464-01, Japan

T. Goto
Department of Electronics, Nagoya University, Nagoya 464-01, Japan

(Received 25 February 1992; accepted for publication 29 April 1992)

A compact interferometer using a grating beamsplitter is reported. The phase of the interference signal was adjusted by using the moire effect of the gratings, so that a small optical path difference was compensated precisely by the magnified displacement of the grating. The optical system was analyzed theoretically on the basis of the Fourier optics. For the interferometric measurement in the microscopic region, a compact optical system was assembled from the microscopic objective and the 25-μm gratings. The characteristics of the proposed interferometer were investigated in the measurements of film thickness, piezoelectric vibration, and photoacoustic effect.

I. INTRODUCTION

For the interferometric measurement in a very small region, several novel optical systems have been proposed.[1–4] Common-path configurations of the optical interferometers are very useful for the measurement of a small optical phase difference since the interference signal is not significantly affected by the external disturbances such as thermal and vibrational effects. The interference signal is especially stable when the differential configuration is used.[2,3,5–7] The two closely spaced spots on the sample surface are illuminated by the split laser beams, so that the long-wavelength acoustic effects causing the relative displacement between the interferometer and sample surface can be eliminated.

As well as the Nomarski interferometer,[2,7,8] the differential interferometer using a grating as the beamsplitter and recombiner is reported to be very stable.[6,8,9] In addition, the optical system of the interferometer can be assembled easily. The vibrational amplitude of an ultrasonic transducer was measured with a precision less than 10^{-3} nm by the interferometer using the grating.[9] More recently, two pairs of beams split by a grating were used for the measurement of the film thickness on a flat substrate.[10] However, since the optical path difference was compensated by the rotation of the optical glass plate inserted between the focusing lens and the sample, it was not easy to miniaturize the interferometer. In addition, the insertion of the tilted glass plate may cause the distortion of the wavefront. On the other hand, in the photoacoustic experiments, a similar grating interferometer was used for the measurements of the thermoelastic deformation of the thin plate[11] and also for the detection of the thermal wave.[12] In those experiments, however, the phase difference was not controlled with any spatial means. More recently, the interferometer using the grating is introduced successfully in the force sensor of the atomic force microscope.[13] However, the characteristics of the interferometer have not been analyzed in detail.

In this paper, the interferometric system using the grating moire effect is analyzed on the basis of the Fourier optics. The phase compensation for several combinations of the diffracted beams is examined. The compact interferometric system was assembled from the 25-μm pitch gratings and the microscopic objective lens. In order to investigate the properties of the proposed interferometer, the measurements of film thickness, piezoelectric vibration, and photothermal effect in a small region were carried out.

II. OPTICAL CONFIGURATION

Figure 1 shows the schematic diagram of the optical system of the interferometer. A collimated laser beam passes through the grating G_1 perpendicularly and it is divided into some order beams by diffraction. The two of the diffracted beams are used as the reference and probe beams of the interferometer, respectively. A convex lens is placed between the grating and the sample. The distance between the lens and the grating is set equal to the focal length of the lens, so that the axis of the divided beams are parallel to that of the incident beam after passing through the lens. The sample is located at a distance equal to the focal length from the lens. Since the divided beams are focused on the sample through the lens, lateral resolution of the interferometer is limited by the numerical aperture of the lens. The beams reflected by the sample pass backward along the path similar to the incident beams. The reflected beams are combined by the grating G_2, which is placed on the same plane as G_1. The grating lines of G_2 are parallel to those of G_1. One of the beams diffracted by G_2 is used to obtain the interference signal. For the measurement of the step height of the film thickness, the sample is translated laterally. For the vibrational measurement in a small region, one beam is on the vibrating area and the other beam is focused on the stationary area.

III. THEORETICAL APPROACH

The general analysis is based on the optical arrangement shown in Fig. 2. For simplicity, we considered the transmission optical system equivalent to the actual reflection system. G_1 and G_2 represent the transmission gratings having the spatial frequency multiple of $1/p$, where p is the

Downloaded 11 Nov 2008 to 130.34.135.83. Redistribution subject to AIP license or copyright; see http://rsi.aip.org/rsi/copyright.jsp

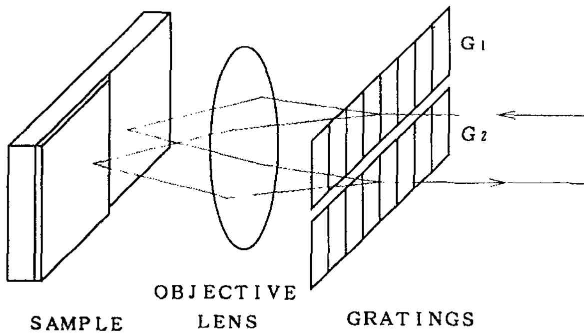

FIG. 1. Schematic diagram of the interferometer.

pitch of the grating. The optical configuration is equal to the Fourier transform system[14] with the grating as object since the gratings and the sample are located in the focal plane of the lenses. In Fig. 2, the sample is shown as the phase object. The amplitude transmittance of the grating G_1 expressed in a Fourier series is given by

$$g_1(x)=\sum_l a_l \exp\left(j2\pi l \frac{x}{p}\right), \tag{1}$$

where a_l and l denote the Fourier coefficient and an integer, respectively. Similarly the amplitude transmittance of the grating G_2 is given by

$$g_2(x)=\sum_m b_m \exp\left(j2\pi m \frac{x-d}{p}\right), \tag{2}$$

where b_m and m denote the Fourier coefficient and an integer, respectively. The relative lateral displacement between the two gratings is represented by d.

Assuming that a plane wave impinges perpendicularly on the grating G_1, the amplitude $U_1(x)$ of the light on the focal plane of the lens L_1 is given by the Fourier transformation of the transmittance $g_1(x)$,

$$U_1(x)=\frac{1}{j\lambda f}\exp(j2kf)\mathscr{F}[g_1(x)], \tag{3}$$

where λ is the wavelength of the laser light. The symbol f is the focal length of the convex lens, and k is equal to $2\pi/\lambda$. Since the transmittance $g_1(x)$ consists of the components having the frequency multiple of $1/p$ as shown by the Eq. (1), $U_1(x)$ given by Eq. (3) expresses the array of

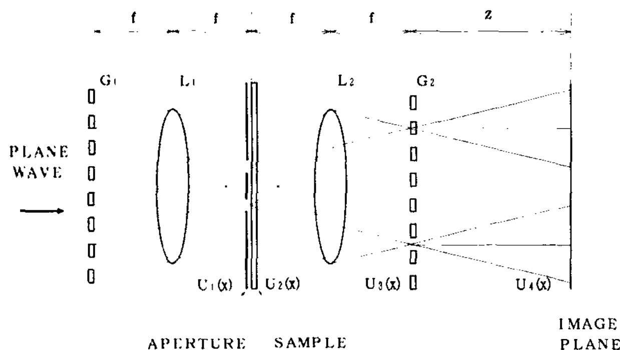

FIG. 2. Schematic diagram of the optical arrangement.

delta functions. As we consider the two beam interferometry, the l_1th and l_2th order beams ($l_1 \neq l_2$) are allowed to pass the sample through the aperture (not shown in Fig. 1). Then, the amplitude $U_1'(x)$ in front of the sample surface is expressed by

$$U_1'(x)=a_{l1}\delta\left(x-l_1\frac{\lambda f}{p}\right)+a_{l2}\delta\left(x-l_2\frac{\lambda f}{p}\right). \tag{4}$$

The two beams pass through the sample with respective phase delays if the phase variation of the sample is not very high. The light amplitude behind the sample is given by

$$U_2(x)=a_{l1}\delta\left(x-l_1\frac{\lambda f}{p}\right)+a_{l2}\delta\left(x-l_2\frac{\lambda f}{p}\right)\exp(j\theta), \tag{5}$$

where the symbol θ is the phase difference between the two beams.

The amplitude $U_3(x)$ at the plane of G_2 is calculated by the Fourier transformation of $U_2(x)$ as

$$U_3(x)=\frac{1}{j\lambda f}\exp(j2kf)\mathscr{F}[U_2(x)]. \tag{6}$$

By passing through the grating G_2, the light beam is diffracted again. The diffracted light is observed at the image plane located at the distance z. When the distance z is much larger than the dimension of the grating G_2, the light amplitude $U_4(x)$ at the image plane is given by the Fraunhofer approximation. We have

$$U_4(x)=\frac{1}{\lambda\sqrt{z}}\exp\left[j\left(kz-\frac{kx^2}{2z}-\frac{\pi}{4}\right)\right]\mathscr{F}[U_3(x)g_2(x)]. \tag{7}$$

Therefore, the light amplitude of the nth order diffraction beam at the image plane is given by

$$U_{4n}=a_{l1}b_{m1}\exp\left(j2\pi m_1\frac{d}{p}\right) + a_{l2}b_{m2}\exp\left[j\left(2\pi m_2\frac{d}{p}-\theta\right)\right], \tag{8}$$

where $m_1=n-l_1$, $m_2=n-l_2$. The intensity of the nth order beam is given by

$$I=|U_{4n}|^2=A+B\cos\left(2\pi(l_1-l_2)\frac{d}{p}-\theta\right), \tag{9}$$

where

$$A=(a_{l1}b_{m1})^2+(a_{l2}b_{m2})^2, \quad B=2a_{l1}a_{l2}b_{l1}b_{l2}. \tag{10}$$

Using Eq. (9), the intensity I was calculated as a function of the displacement d with the phase difference θ as a parameter. Figures 3(a) and 3(b) show the results obtained for the combination of first ($l_1=1$) and zeroth ($l_2=0$ order beams and that of $\pm$1st ($l_1=1$, $l_2=-1$) order beams, respectively. The intensity of the interference signal is assumed to be measured by zeroth order beam diffracted by $G_2(n=0)$. We further assume that the gratings have the binary transmittance with a duty cycle equal to 1/2 when

Downloaded 11 Nov 2008 to 130.34.135.83. Redistribution subject to AIP license or copyright; see http://rsi.aip.org/rsi/copyright.jsp

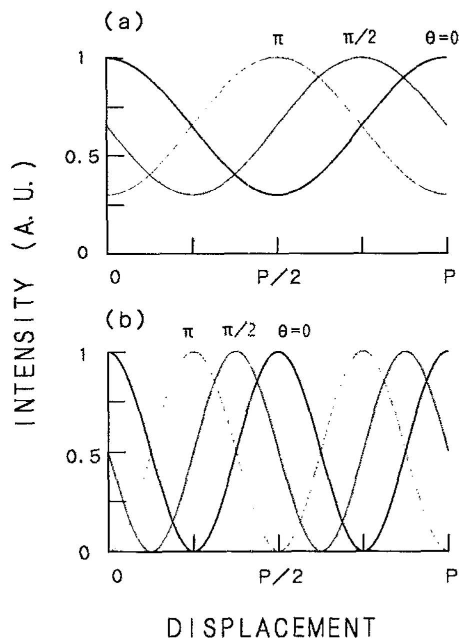

FIG. 3. Interference signals calculated as a function of the grating displacement d with phase difference θ as a parameter. (a) the combination of zeroth and first order beams. (b) the combination of ±first order beams.

we calculate the interference intensity. The intensity calculated for the combination of first and zeroth order beams varies with the period of p for the increase of displacement d as shown in Fig. 3(a). Unlike this, the intensity for the combination of ±first order beams changes with the period of $p/2$ as shown in Fig. 3(b). On the other hand, the intensity of the interference signal changes with the period of 2π for the increase of θ for any combination of the diffracted beams.

The phase difference θ of interference signal is related to the optical path difference ΔL by the equation $\theta = 2\pi\Delta L/\lambda$. In the conventional two-beam interferometer, the path difference ΔL is usually compensated with the displacement of the mirror equal to $\Delta L/2$. In our grating interferometer, however, the path difference ΔL is compensated with the magnified displacement $\Delta L(p/\lambda)$ of G_2 for the combination of zeroth and first beams. And for the combination of first order beams, the path difference ΔL can be compensated by a half $\Delta L(p/2\lambda)$ of the lateral displacement used for the combination of zeroth and first order beams. Therefore, the phase can be adjusted with a high precision by the magnified displacement.

The intensities of the interference signals have been investigated theoretically for the other combinations of the diffracted beams. The results are summarized in Table I. The lateral displacement d_L of G_2 necessary for the compensation of the optical path difference ΔL, the average intensity I_{av}, and the contrast C of the interference signal are listed for the combination of l_1th and l_2th order beams. Furthermore, we have examined the characteristics of the interference signals for different transmittance of the gratings. Although the values of I_{av} and C are different from those shown in the Table I, the lateral displacement d_L is unchanged.

TABLE I. Characteristics of the interferometer signals for the different combinations of the diffracted beams. l_1,l_2 denote the orders of the beams diffracted from the grating G_1. d_L is the lateral displacement of the grating G_2 necessary for the compensation of the optical path difference L. I_{av} and C are the mean intensity and the contrast of the interference signal, respectively.

l_1	l_2	d_L	I_{av}(a.u.)	C(%)
0	1(−1)	$\Delta LP/\lambda$	10.0	70
0	3(−3)	$\Delta LP/3\lambda$	8.5	9
1	−1	$\Delta LP/2\lambda$	2.9	100
1	3	$\Delta LP/2\lambda$	1.4	22
1	−3	$\Delta LP/4\lambda$	1.4	22
3	−3	$\Delta LP/6\lambda$	0.3	100

IV. EXPERIMENTAL APPARATUS

Figure 4 shows the schematic diagram of the optical head of the interferometer. The optical head is composed of the optical microscope objective (Olympus 10×) and the two binary transmission gratings with 25-μm pitch. The distance from the front end of the objective to the sample surface, which corresponds to the front focal plane of the objective, is equal to 6 mm. The two gratings are placed in the rear focal plane of the objective, which is nearly equal to the rear surface of the objective lens. Therefore, the optical head of the interferometer is as small as the microscopic objective. Since we use the binary transmission grating with the duty cycle equal to 1/2, the intensities of light beams diffracted into zeroth and first orders are prominent. In order to use two of them for the interferometric measurement, one of the beams is stopped

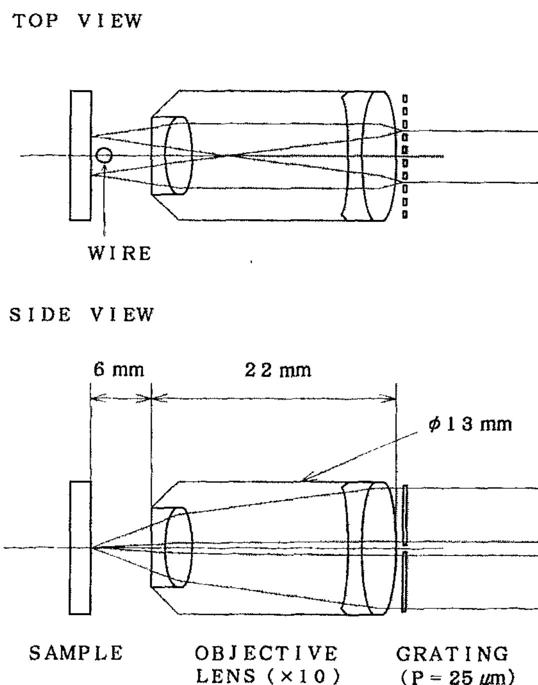

FIG. 4. Schematic diagram of the optical head of the interferometer.

Downloaded 11 Nov 2008 to 130.34.135.83. Redistribution subject to AIP license or copyright; see http://rsi.aip.org/rsi/copyright.jsp

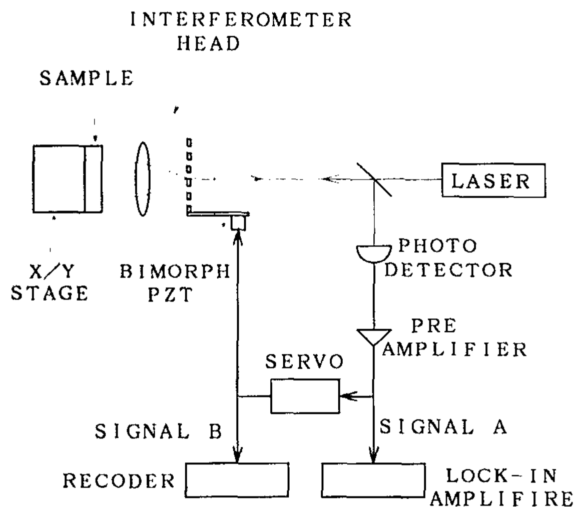

FIG. 5. Schematic diagram of the experimental setup.

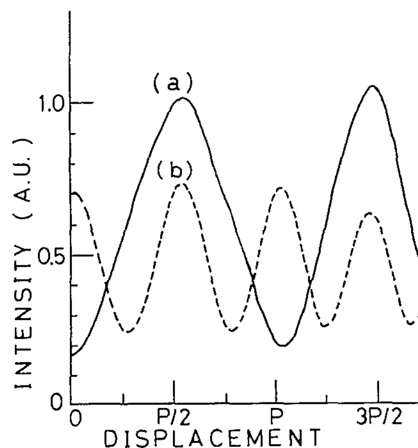

FIG. 6. Interference signals as a function of the lateral displacement d of G_2. (a) the combination of zeroth and first order beams. (b) the combination of $\pm$first order beams.

with a thin wire as shown in Fig. 4. (In Fig. 4, the zeroth order beam is stopped.) The distance between the zeroth and first order beams on the sample surface is approximately 0.5 mm.

Figure 5 shows the schematic diagram of the interferometer system. A He–Ne laser (Uniphase, 1107 P, $\lambda=633$ nm, 0.8 mW) is used as the light source. We use the combination of zeroth and first order beams and that of $\pm$first order beams in the experiments. The grating G_2 (Fig. 1) in the interferometer is translated laterally by the PZT bimorph (Tokin, NLB-33$\times$11$\times$1). The sample is held on the X-Y stage driven by pulse motor with the accuracy of 1 μm. The interference signal is measured by a photodiode. The output of the photodiode is fed to the low-frequency servo control circuit to keep the dc signal level constant by moving the grating with PZT bimorph. By keeping the dc level of the signal at a given voltage (for example, at the midpoint between the maximum and minimum of the interference signal), phase change of the interference signal at low frequency is compensated by the translation of the grating. For the low-frequency measurement such as slow displacement sensing, the phase change is measured from the output of the servo control circuit (signal B). The response time in signal B is longer than 1 s, which is mainly determined by that of servo control circuit. For the high-frequency measurement such as vibration sensing, the low-frequency servo control circuit is used for the compensation of the long time-range drift due to thermal expansion. Therefore the sensitivity for the signal at the high frequency is kept unchanged. We use signal A to measure the vibrational amplitude and signal B to obtain the surface profile of the sample.

V. DISPLACEMENT AND SURFACE PROFILE MEASUREMENT

The characteristics of the grating interferometer were examined in the following experiments. The intensity signals of the interferometer were measured by changing the lateral displacement d of G_2. Figures 6(a) and 6(b) show the results obtained for the combination of first and zeroth order beams and that for $\pm$ first order beams, respectively. The intensity signals of the interferometer change with the periods of p and $p/2$ for the increase of d as shown in Figs. 6(a) and 6(b). These experimental results are explained well by the theoretical calculations shown in Fig. 3 and Table I.

Next, the stability and sensitivity for the displacement are examined and the results are shown in Fig. 7. A flat

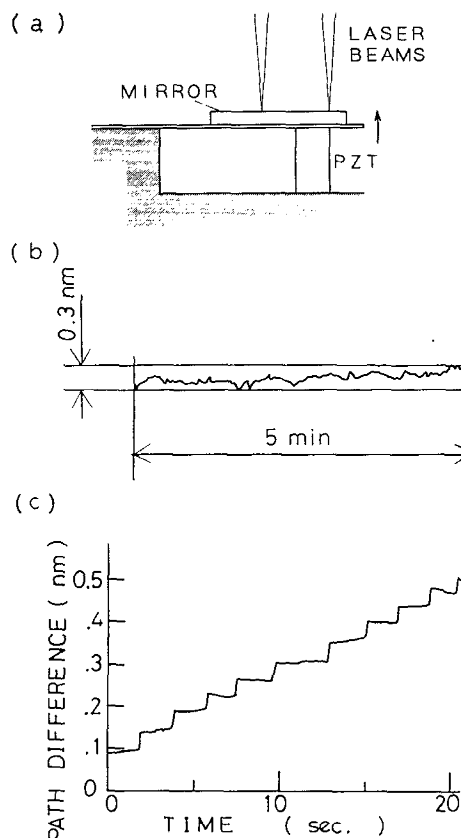

FIG. 7. (a)Schematic diagram of experimental arrangement. (b) Drift of the interference signal measured as a function of the time. (c) Interference signal for the step changes of the path difference measured as a function of time.

Downloaded 11 Nov 2008 to 130.34.135.83. Redistribution subject to AIP license or copyright; see http://rsi.aip.org/rsi/copyright.jsp

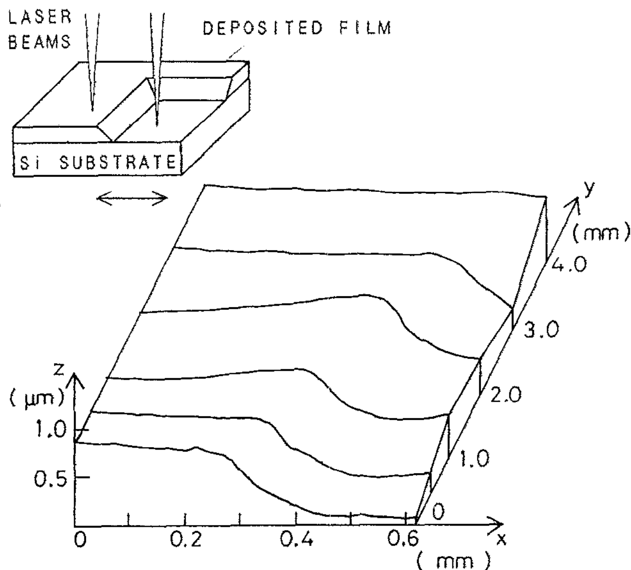

FIG. 8. The measured surface profile of the deposited film.

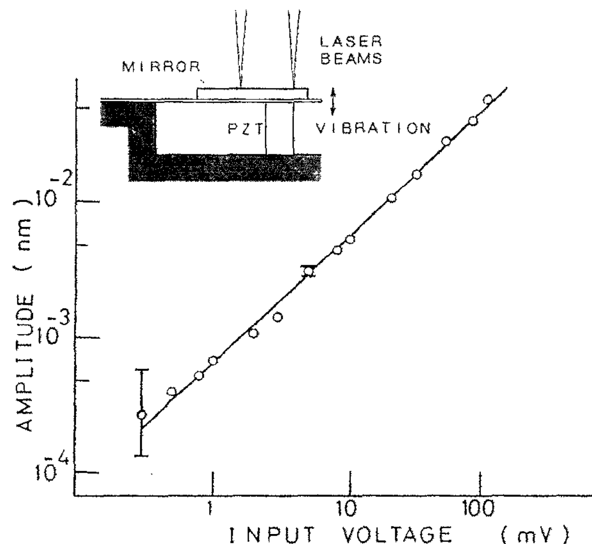

FIG. 9. Amplitude signal of the vibration of the mirror sample measured as a function of the ac voltage applied to the PZT element.

mirror was placed at the front focal plane of the lens and the differential displacements were measured using the experimental arrangement shown in Fig. 7(a). Figure 7(b) shows the intensity signal of the interferometer as a function of the measurement time without applying the voltage to the PZT element. The drift rate of the interferometer was evaluated from the repeated measurements to be less than 10^{-3} nm/s. Figure 7(c) shows the step change of the path difference. The flat mirror was tilted with PZT element by a step of 0.03 nm and signal A was measured by the recorder without the servo control. Before the measurement, the dc level of signal A was set to a midpoint between the maximum and minimum of the interference signal. The time constant of the measurement system was approximately 0.1 s, which was determined by the response time of the recorder. The sensitivity for the measurement of the static displacement was estimated to be 0.01 nm or less under our experimental conditions.

On the other hand, the signals varied sinusoidally for a large tilt in the experimental arrangement shown in Fig. 7(a). One period of the signal corresponded to the differential displacement of $\lambda/2$ for the both combinations of the two beams. Hence, it was confirmed that the path differences equal to λ were compensated by the grating displacement of p and $p/2$ for the combination of first and zeroth order beams and that for $\pm$ first order beams, respectively.

In the next experiment, the measurement of the surface profile was carried out. The plasma polymerized film was deposited on the Si substrate. A part of the substrate was covered before deposition to make a step change of the film thickness (Fig. 8). The surface of the sample was covered by the evaporated aluminum after the deposition. The surface profile of the film was measured by translating the sample laterally and by measuring the control signal of the PZT bimorph (signal B). One of the laser beams was located on the substrate and the other was translated across the step change of the film thickness. We used the combination of the $\pm$first order beams for the measurement. The control signal of the PZT bimorph (signal B), which was corresponding to the displacement of the grating, was converted to the film thickness of the sample. And the results are shown in Fig. 8. The sample was translated in the directions of X and Y axes and two-dimensional distribution of the film thickness was measured. The averaged value of the measured thickness of the film was 750 ± 40 nm. The uncertainty of the measured thickness was mainly caused by roughness of the deposited film.

VI. VIBRATIONAL MEASUREMENTS

In order to measure the vibrational amplitude much smaller than the wavelength, we carried out two kinds of experiments. In the first experiment, the vibration of the PZT element was examined. The measurement was carried out under the phase conditions that the maximum slope of the intensity as a function of the optical path difference was obtained. The conditions corresponded to the midpoints between the maxima and minima of the interference intensity, and they were obtained by adjusting the lateral position of G_2. The differential intensity ΔI of the interferometer is proportional to a small displacement $\Delta L/2$ under the conditions:

$$\Delta I=\frac{4\pi B}{\lambda}\frac{\Delta L}{2}. \tag{11}$$

Here B is given by Eq. (10). Figure 9 shows the schematic diagram of the experimental arrangement and the vibrational amplitude measured as a function of the ac voltage (100 Hz) applied to the PZT element. The signal A in Fig. 5 was measured by the lock-in amplifier in the frequency bandwidth of 0.125 Hz. The absolute value of the vibrational amplitude was obtained from Eq. (11). Decreasing the voltage, the vibrational amplitude decreases linearly. The amplitude less than 1×10^{-3} nm is measured in the experiment as shown in Fig. 9.

Downloaded 11 Nov 2008 to 130.34.135.83. Redistribution subject to AIP license or copyright; see http://rsi.aip.org/rsi/copyright.jsp

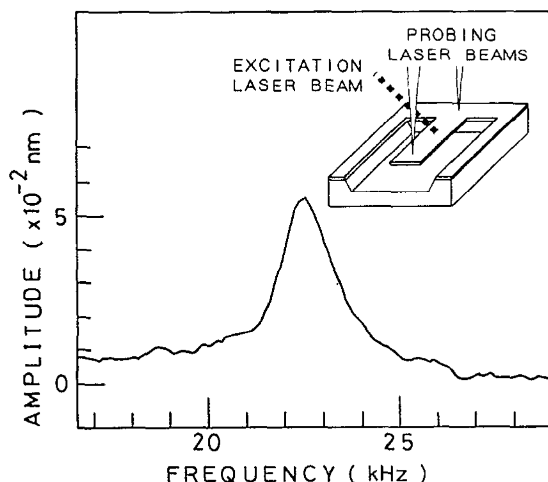

FIG. 10. Amplitude signal of the vibration of the microcantilever measured as a function of the frequency. The vibration is excited by the photoacoustic effect.

Recently, the interferometer was successfully employed in the photoacoustic and photothermal techniques since it made the technique noncontact and sensitive at high-frequency region. In our second experiment, the interferometer was used for the sensing of the photoacoustic effect. Here, we demonstratively measured the photoacoustic vibration of the microcantilever in the atmospheric air. The cantilever was made of SiO_2 by the lithography process.[15] The length, width, and thickness of the cantilever were approximately 200, 20, and 1 μm, respectively. The surface of the cantilever was coated with aluminum. Figure 10 shows the vibrational amplitude of the cantilever as a function of the frequency around the lowest resonant frequency (22.5 kHz) of the cantilever. The maximum value of the vibrational amplitude was evaluated to be 0.05 nm. From this experiment, it is shown that the proposed interferometer is also useful for the photoacoustic measurements.

VII. DISCUSSION

A compact grating interferometer was developed for the measurement of a small phase change in the microscopic region. Using the moire effect of the gratings, the optical path difference was compensated by the magnified displacement of the grating. The proposed interferometer was analyzed on the basis of the Fourier optics. And the phase change due to the translation of the grating was investigated for the several combinations of the diffracted beams. A compact interferometer head was constructed (less than 30 mm in length) by using a microscopic objective and the 25-μm pitch gratings.

Using the PZT element, the sensitivity of the displacement measurement was evaluated to be the order of 10^{-2} nm. The vibrational measurement was carried out by using a lock-in amplifier and the sensitivity less than 10^{-3} nm was obtained. In addition, the step height of the thickness of the plasma polymerized film and the small vibration of the microcantilever activated by the photoacoustic effect were measured. The fact that the proposed interferometer has a compact differential configuration makes it useful for the interferometric measurements in microscopic region.

[1] D. C. Leiner and D. T. Moore, Rev. Sci. Instrum. **49**, 1702 (1978).
[2] G. Makosch and B. Drollinger, Appl. Opt. **23**, 4544 (1984).
[3] C. W. See, M. V. Iravani, and H. K. Wickramasinghe, Appl. Opt. **24**, 2373 (1985).
[4] B. Bhushan, J. C. Wyant, and C. L. Koliopoulos, Appl. Opt. **24**, 1489 (1985).
[5] V. T. Chitnis, Y. Uchida, K. Matsuura, and S. Hattori, Opt. Laser Technol. **15**, 269 (1983).
[6] K. Hane, K. Yoneda, and S. Hattori, Opt. Laser Technol. **17**, 208 (1985).
[7] J. T. Fanton and G. S. Kino, Appl. Phys. Lett. **51**, 66 (1987).
[8] G. Nomarski, J. Phys. Radium **16**, 95 (1955).
[9] K. Yoneda, M. Tawata, and S. Hattori, Jpn. J. Appl. Phys. **20**, Suppl. 20-3, 61 (1981).
[10] V. T. Chitnis, Y. Uchida, K. Hane, K. Yoneda, and S. Hattori, Jpn. J. Appl. Phys. **25**, 1078 (1986).
[11] K. Hane, T. Naito, and S. Hattori, Appl. Opt. **30**, 72 (1991).
[12] H. G. Walther, K. Friedrich, K. Haupt, K. Muratikov, and A. Glazov, Appl. Phys. Lett. **57**, 1600 (1990).
[13] S. Watanabe, K. Hane, and T. Goto, J. Vac. Sci. Technol. B **10**, 7 (1992).
[14] J. W. Goodman, *Introduction to Fourier Optics* (McGraw-Hill, New York, 1968).
[15] E. Bassous, IEEE Trans. Electric Devices **ED-25**, 1178 (1978).

Downloaded 11 Nov 2008 to 130.34.135.83. Redistribution subject to AIP license or copyright; see http://rsi.aip.org/rsi/copyright.jsp